

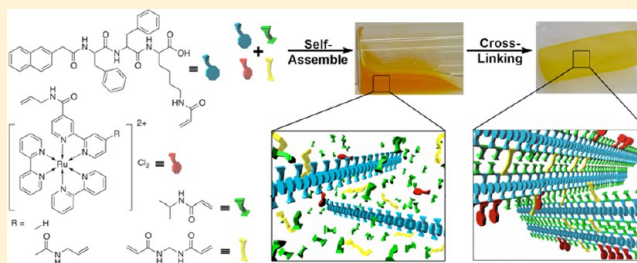
Post-Self-Assembly Cross-Linking to Integrate Molecular Nanofibers with Copolymers in Oscillatory Hydrogels

Ye Zhang, Rong Zhou, Junfeng Shi, Ning Zhou, Irving R. Epstein,* and Bing Xu*

Department of Chemistry, Brandeis University, 415 South Street, Waltham, Massachusetts 02454, United States

S Supporting Information

ABSTRACT: We study the use of post-self-assembly cross-linking to combine molecular nanofibers of hydrogelators with copolymers to generate oscillatory materials using the Belousov–Zhabotinsky reaction. The formation of nanofibers from designed hydrogelators provides multiple polymerizable sites for copolymerizing with *N*-isopropylacrylamide and for attaching a catalytic ruthenium bipyridine complex on the copolymer. The combination of supramolecular self-assembly with copolymerization offers a versatile and facile approach for generating soft materials that have large pores in the gel network and robust mechanical integrity. These larger pores facilitate the diffusion of the reactants and accelerate the chemical oscillation by about a factor of 4 relative to a poly(NIPAAm–Ru) gel that contains no molecular nanofibers.



INTRODUCTION

This article reports a systematic investigation of the use of post-self-assembly cross-linking¹ to combine molecular nanofibers of hydrogelators^{2–11} with copolymers to form polymeric hydrogels as a new type of oscillatory material. Chemical oscillation, the spontaneous, periodic, or nearly periodic, variation of chemical concentrations in time and/or space, represents a classic example of nonequilibrium chemical dynamics.^{12,13} The most studied, and most robust, oscillating chemical reaction is the Belousov–Zhabotinsky (BZ) reaction, the bromate oxidation of an organic substrate catalyzed by a metal ion or metal complex.¹⁴ The BZ reaction provides a model system to mimic a variety of complex processes, such as biological morphogenesis, in monodisperse microemulsions.¹⁵ In heterogeneous systems it facilitates investigation of the role of reaction-diffusion in pattern formation under conditions that are more relevant to morphogenesis,^{16,17} and it can be used to develop chemomechanical systems.^{19,20}

Among the heterogeneous or discontinuous systems used for exploring chemical oscillation, soft materials, such as gels, provide several distinct advantages over other heterogeneous or discontinuous systems¹⁸ such as surfaces, ion-exchange resins, membranes, and microemulsions. For example, in addition to minimizing the hydrodynamic effects and formation of bubbles that usually occur in homogeneous aqueous systems, gels are able to immobilize, stabilize, and even control the spatial distribution of catalyst in the BZ reaction.²¹ Yoshida et al.¹⁹ first demonstrated the use of a chemical oscillator to generate mechanical oscillation by making a copolymer gel consisting of *N*-isopropylacrylamide (NIPAAm) and the BZ catalyst Ru(bpy)₃²⁺,^{22,23} which generated a swelling–deswelling oscillation of the gel when it was immersed in a solution containing the BZ reactants. Because it contains a thermosensitive poly(NIPAAm)

structure,²⁴ the poly(NIPAAm-co-Ru(bpy)₃²⁺) gel undergoes a cyclic swelling–deswelling alteration when Ru(bpy)₃ⁿ⁺ (*n* = 2 or 3) is periodically oxidized and reduced in the BZ reaction at constant temperature. Despite this seminal work, perhaps because of the lack of a general and facile approach to generate new molecular arrangements and to vary the distribution of catalyst within a gel, only a handful of studies^{1,25–28} have focused on controlling the physical network structure of gels to tailor their properties and on understanding the correlation between molecular structure, chemical oscillation, and mechanical actuation.

In our previous work,¹ we used molecular self-assembly as a new approach to introduce ordered nanostructures into hydrogels²⁹ that undergo chemical oscillation. Specifically, we prepared a small peptide hydrogelator with a polymerizable group and used its self-assembled nanofibers to copolymerize with a ruthenium complex containing a vinyl group. This post-self-assembly cross-linking approach not only demonstrated the stability of the peptide bond under the rather severe conditions (e.g., oxidative and acidic) of the BZ reaction, but also pointed toward a feasible way to employ sophisticated peptide motifs in hydrogels for generating chemical oscillation. Moreover, this post-self-assembly cross-linking approach offers an opportunity to generate a series of different molecular structures for understanding the correlation between chemical oscillation and molecular organization.

Here we systematically examine several hydrogels produced by this post-self-assembly cross-linking approach. We synthesize and characterize oscillatory hydrogels made by varying the

Received: February 6, 2013

Revised: May 6, 2013

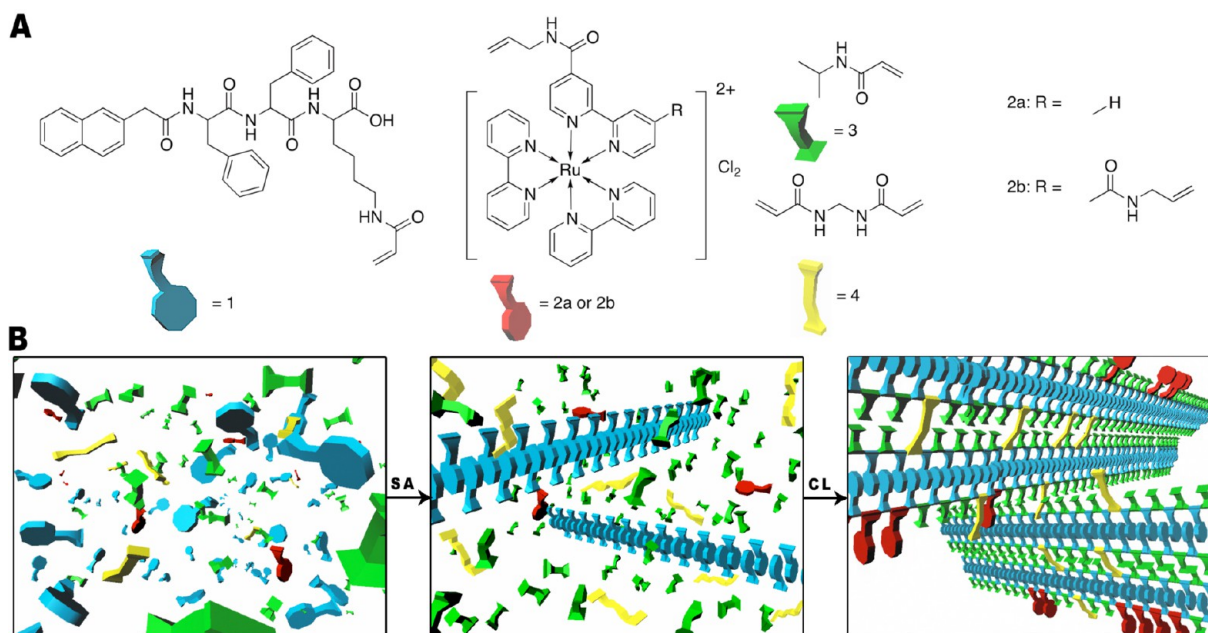


Figure 1. (A) Molecular structures of the hydrogelator bearing a polymerizable group (**1**), two catalysts of the Belousov–Zhabotinsky (BZ) reaction (**2a**, **2b**), NIPAAm monomer (**3**), and the cross-linker, *N,N'*-methylenebis(acrylamide) (BIS, **4**). (B) Schematic illustration of the post-self-assembly cross-linking process for making the polymeric gel network for chemical oscillation (SA = self-assembly; CL = cross-linking).

relative amounts of the polymerizable supramolecular hydrogelator, the NIPAAm monomer, the polymerizable ruthenium bipyridine complex, and the *N,N'*-methylenebis(acrylamide) (BIS) cross-linker. We also use a polymerizable ruthenium bipyridine complex containing two vinyl groups, which can act both as a catalyst and as a cross-linker for formation of the oscillatory hydrogel. Although our results indicate that both the type of catalyst and the amount of cross-linker affect the frequency of chemical oscillation in the gels, the influences of the catalyst and cross-linker are rather small, because the molecular self-assembly controls the mean pore size of the hydrogel network, which dictates the reaction-diffusion behavior of the BZ reagents. Oscillation with a ruthenium catalyst containing two allylformamide groups is faster, both in solution and in gel, than with a ruthenium catalyst containing only one allylformamide group. When the amount of cross-linkers increases, the chemical oscillation of the gel slows. Our results also suggest that the nanofibers formed by self-assembly exert the primary influence on the period of chemical oscillation, since inclusion of the NIPAAm monomer has little effect on the oscillation period. This work illustrates a new approach to effectively control the pore sizes of the networks in BZ gels and provides new insights for modulating the behavior of an oscillatory chemical system.

EXPERIMENTAL SECTION

General Synthetic Methods and Materials. The polymerizable supramolecular hydrogelator **1** and the ruthenium complexes **2a**, **2b**, shown in Figure 1, were synthesized according to previously published procedures.^{1,30,31} The organic solvents used in this experiment, methylene chloride, methanol, and chloroform, were HPLC grade (Fisher). Ethanol and acetone were GC grade (Fisher). Anhydrous DMF (99.8%), 4,4'-dimethyl-2,2'-bipyridine (99.5%), *N,N'*-dicyclohexylcarbodiimide (DCC) (99.0%), 1-ethyl-3-(3-dimethylaminopropyl) carbodiimide (EDC), allylamine (99.0%), and *cis*-bis(2,2'-bipyridine)dichlororuthenium(II) hydrate (97%) were

purchased from Sigma-Aldrich. *N*-Hydroxysuccinimide (NHS) and hydroxybenzotriazole (HOBt) were purchased from GL Biochem. The *N,N'*-methylenebis(acrylamide) (BIS) cross-linker **4** and the *N*-isopropylacrylamide (NIPAAm) monomer **3** were purchased from Fisher. All reagents were used as received unless otherwise noted. NMR spectra were measured on a 400 MHz Varian NMR spectrometer in DMSO-*d*₆.

Nap-FFK-Acrylic Acid (1**).** We made the peptide hydrogelator NapFFK³² (nap = naphthalene, F = phenylalanine, K = lysine) using solid phase synthesis. In the following liquid-phase reaction, assisted by NHS and EDC, we coupled NapFFK (502 mg, 0.825 mmol) with acrylic acid (0.55 mL, 8.25 mmol) in acetone–water solvent (pH = 8–9). After the workup and purification, we obtained **1** in 62% yield.¹

Ru(II)(2,2'-bipyridine)₂(*N*-allyl-[2,2'-bipyridine]-4-carboxamide)dichloride (2a**).** **2a** was synthesized according to the reported procedure.¹

Ru(II)(2,2'-bipyridine)₂(*N*-allyl-[2,2'-bipyridine]-4,4'-carboxamide)dichloride (2b**).** 2,2'-Bipyridine-4,4'-dicarboxamide (200 mg, 0.82 mmol), HOBt (266 mg, 1.97 mmol), and EDC (306 mg, 1.97 mmol) were charged into a 25 mL round-bottom flask. DMF (3 mL) and THF (9 mL) were added to the flask. The mixture was stirred at room temperature while DIEA (0.57 mL, 3.28 mmol) was introduced into the mixture. After that, allylamine (0.2 mL, 2.46 mmol) was added to the mixture. The reaction was heated to 60 °C and stirred overnight. After removal of most of the solvent from the reaction mixture, water was added to the flask to give a white precipitate. The target compound, *N,N'*-diallyl-[2,2'-bipyridine]-4,4'-dicarboxamide, was obtained in 90% yield by collecting the precipitate.

Ethanol (4.5 mL) and water (0.5 mL) were introduced into a 10 mL round-bottom flask charged with *N,N'*-diallyl-[2,2'-bipyridine]-4,4'-dicarboxamide (90 mg, 0.28 mmol) and Ru(bipy)₂Cl₂ (144 mg, 0.28 mmol). The solution was degassed with nitrogen for 30 min. Then it was heated at 90 °C overnight. The pure Ru complex **2b** was obtained after column

chromatography (Sephadex LH 20) as a dark red powder in 90% yield.

Synthesis of Hydrogel IA. After adding **1** (2.93 mg) and **2a** (0.27 mg) to water (850 μ L), we adjusted the pH to 9 to form Gel IA by the self-assembly of **1**. After the hydrogel was degassed with N₂, we added V₅₀ (2,2'-azobis(2-methylpropionamidine)-dihydrochloride) at 0.2 wt % of all compounds to the hydrogel as the initiator for photopolymerization. The mixture was poured into a glass mold and sealed for UV irradiation (mercury lamp) for 20 min to produce a cross-linked hydrogel, C-Gel IA. The C-Gel IA underwent dialysis for 3 days to remove the initiators and any unreacted monomer. Finally, the C-Gel IA was immersed in a saturated KPF₆ solution for 3 days to exchange the anions from Cl[−] to PF₆[−].

Synthesis of Hydrogel IB. The procedure is similar to the synthesis of Gel IA and C-Gel IA, except that **1** (2.93 mg), **2a** (0.27 mg), and **4** (1.4 mg) were added to the water (850 μ L).

Synthesis of Hydrogel IC. The procedure is similar to the synthesis of Gel IA and C-Gel IA, except that **1** (2.93 mg), **2a** (0.27 mg), and **3** (2.4 mg) were added to the water (850 μ L) for the self-assembly and polymerization.

Synthesis of Hydrogel ID. The procedure is similar to the synthesis of Gel IA and C-Gel IA, except that **1** (2.93 mg), **2a** (0.27 mg), **3** (2.4 mg), and **4** (1.4 mg) were added to the water (850 μ L).

Synthesis of Hydrogels IIA, IIB, IIC and IID. The procedures are similar to those for making the type I hydrogels, except that **2b** replaces **2a**.

RESULTS AND DISCUSSION

Molecular Design. To obtain oscillatory hydrogels with ordered structures, we exploit the fact that molecular self-assembly of the hydrogelator takes place in water to make ordered nanostructures in either the presence or the absence of the NIPAAm monomer (**3**). We then cross-link the monomer and/or the ruthenium catalysts to the molecular nanofibers. As shown in Figure 1, the designed hydrogelator (**1**) consists of a molecular motif (NapFF) that is known to favor self-assembly in water,²⁹ a lysine residue, and a polymerizable acrylic amide. We design two kinds of polymerizable catalysts: **2a** and **2b**. While **2a** contains one vinyl group, **2b** bears two vinyl groups. Thus, **2b** can itself act as a cross-linker for making the hydrogel network. Since **2a** is unable to serve as a cross-linker, we introduce BIS (**4**) as the cross-linker when **2a** is the catalyst for the BZ reaction. By varying the relative amounts of **1**, **2**, **3**, and **4**, we obtain a series of hydrogels, which have different compositions and structures in their gel matrices, and we study their oscillatory behavior.

Synthesis of the Hydrogels. As shown in Figure 1B, the process of synthesizing the hydrogels consists of two major steps—self-assembly and polymerization/cross-linking. During the self-assembly process, the peptide hydrogelators (**1**) self-assemble in water in the presence of the ruthenium complexes (**2a** or **2b**), the monomer (**3**), and/or the cross-linker (**4**). Since the structure of **1** differs drastically from those of the other compounds (i.e., **2a**, **2b**, **3**, and **4**), the self-assembly of **1** is largely independent of the presence of those species. After the self-assembly, the addition of the polymerization initiator to the hydrogel allows the polymerization of the molecules containing vinyl groups to form cross-linked networks. Because **1** self-assembles in water to form nanofibers, the polymerization fixes the nanofibers and allows other compounds to be incorporated into those nanofibers. Table 1 summarizes the

Table 1. Amounts of Peptide Hydrogelator, Ruthenium Complexes, NIPAAm, and Cross-Linker BIS in the BZ Gels, Diameters of the Nanofibers, And Periods of Chemical Oscillation

gel	composition (mg)					diameter (nm)		period (s)
	1	2a	2b	3	4	SA ^a	CL ^b	
IA	2.93	0.27	-	-	-	10.6	12.9	53
IB	2.93	0.27	-	-	1.4	10.0	9.4	56
IC	2.93	0.27	-	2.4	-	10.1	13.6	52
ID	2.93	0.27	-	2.4	1.4	13.0	16.1	56
IIA	2.93	- ^c	0.27	-	-	/ ^d	/	45
IIB	2.93	-	0.27	-	1.4	/	/	53
IIC	2.93	-	0.27	2.4	-	/	/	x ^e
IID	2.93	-	0.27	2.4	1.4	/	/	x

^aAverage diameter of self-assembled nanofibers before cross-linking.

^bAverage diameter of self-assembled nanofibers after cross-linking.

^cAbsence: -. ^dNot measured: /. ^eNo chemical oscillation: x.

compositions of the hydrogels made in this work, which contain the same amount of the hydrogelator but different amounts of the other components. The hydrogels we examine are of two types: Type I hydrogels contain the ruthenium complex **2a** as the catalyst of the BZ reaction; type II hydrogels employ **2b**, which not only serves as the BZ catalyst, but also as the cross-linker of the polymer network. To assess the effects of the monomer **3** and the cross-linker **4**, we consider four gels of each type: A, without **3** and **4**; B, without **3**; C, without **4**; and D, with **3** and **4**.

By mixing **1** and **2a** in water and adjusting the pH to 9, we obtain a weak hydrogel, Gel IA, which barely supports its own weight (Figure 2A). The formation of the hydrogel suggests that the molecules of **1** self-assemble in water to form nanofibers. Transmission electron microscopy (TEM) confirms that Gel IA consists of a network of nanofibers, which have rather uniform diameters of 11 ± 2 nm. Most of the pores of the network are less than 100 nm in diameter. UV irradiation in the presence of initiator V₅₀ polymerizes **1** in the nanofibers and allows the attachment of the BZ catalyst to the nanofibers. After polymerization, the soft gel becomes a thin film (Figure 2C). TEM reveals that the mean width of the nanofibers increases to 13 ± 2 nm. Some segments of the nanofibers become thicker than others (Figure 2D), which probably results from attachment of **2**, though self-polymerization of the hydrogelators is also possible. Although there are more entanglements and bends of the nanofibers after polymerization, the nanofibers remain distinct and form a network with typical pore size larger than before the polymerization.

The addition of cross-linker **4** to a mixture of **1** and **2a** in water at pH 9 affords Gel IB, shown in Figure 3A, as a weak hydrogel. TEM of Gel IB shows that self-assembly of molecule **1** in water forms the nanofibers. The nanofibers of Gel IB are very much like those in Gel IA. For example, they have similar width (average diameter 10 ± 2 nm) and a parallel arrangement (Figure 3B). The pores of the network in Gel IB are bigger than those in Gel IA, but still under 100 nm. After applying the initiator V₅₀ and UV irradiation, we obtain the cross-linked hydrogel C-Gel IB that consists of the BZ catalyst and cross-linker attached to the nanofibers. Through copolymerization, the soft hydrogel turns into a thin film of C-Gel IB. TEM shows that C-Gel IB (Figure 3C) consists of nanofibers with nodes and short branches along them, resulting from the cross-linking of **2a** and **4**. The width of the nanofibers remains almost the

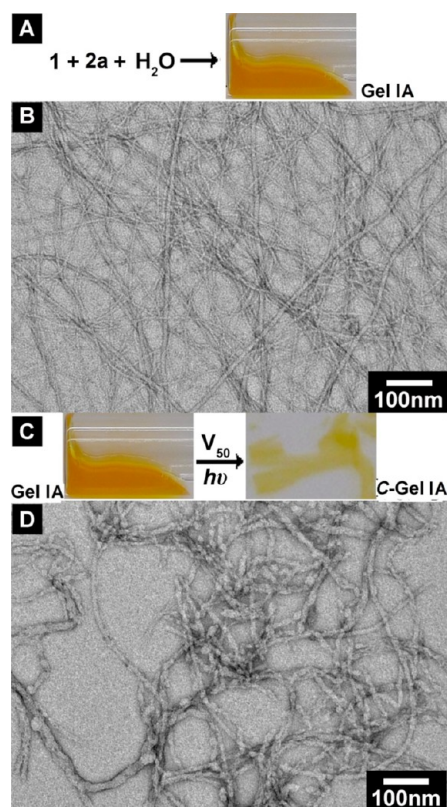


Figure 2. (A) Process for making molecular hydrogel (Gel IA) by self-assembly of **1** after addition of **1** and **2a** to water and adjustment of the pH to 9. (B) TEM image of Gel IA. (C) Process for making cross-linked hydrogel C-Gel IA by addition of V_{50} (0.0064 mg) to the mixture with subsequent UV irradiation for 20 min. (D) TEM image of the polymerized cross-linked gel (C-Gel IA).

same (9 ± 2 nm) as before polymerization (Figure 3D), suggesting that there is limited shrinkage of the nanofibers of the hydrogelators during polymerization and cross-linking. Scanning electron microscopy (SEM) of C-gel IB shows that the surface of the hydrogel is sponge-like and that the pores of the network are about 150–250 nm in diameter (Figure 3E).

We mixed **1**, **2a**, and monomer **3** in water to make the weak hydrogel Gel IC by adjusting the pH to 9 (Figure 4A). Gel IC and the control Gel IA differ very little either in the width of their nanofibers (10 ± 2 nm) or the parallel arrangement of the nanofibers (Figure 4B). The BZ catalyst attaches to the nanofibers when the polymerization occurs under UV irradiation in the presence of the V_{50} initiator. The thin film gel (Figure 4C) after the copolymerization consists of nanofibers with a few nodes and branches along their length. The width of the nanofibers increases to 13 ± 2 nm, suggesting that the cross-linking process recruits significant amounts of hydrogelators and acrylic amide monomers from the solution phase to the nanofibers, which form a relatively loose network with pores that are slightly larger than 100 nm (Figure 4D).

By mixing **1**, **2a**, **3**, and **4** in the water and adjusting the pH to 9, we obtain Gel ID (Figure 5A) and examine it with TEM. The mean width of the nanofibers (Figure 5B) of Gel ID increases from around 10 to 13 nm. The nanofibers are also more distinct with pore sizes less than 100 nm. UV irradiation of Gel ID in the presence of V_{50} produces a thin film gel C-Gel ID (Figure 5C). The cross-linking effect is clearly enhanced by the presence of **2a** and **4** and leads to a significant increase in

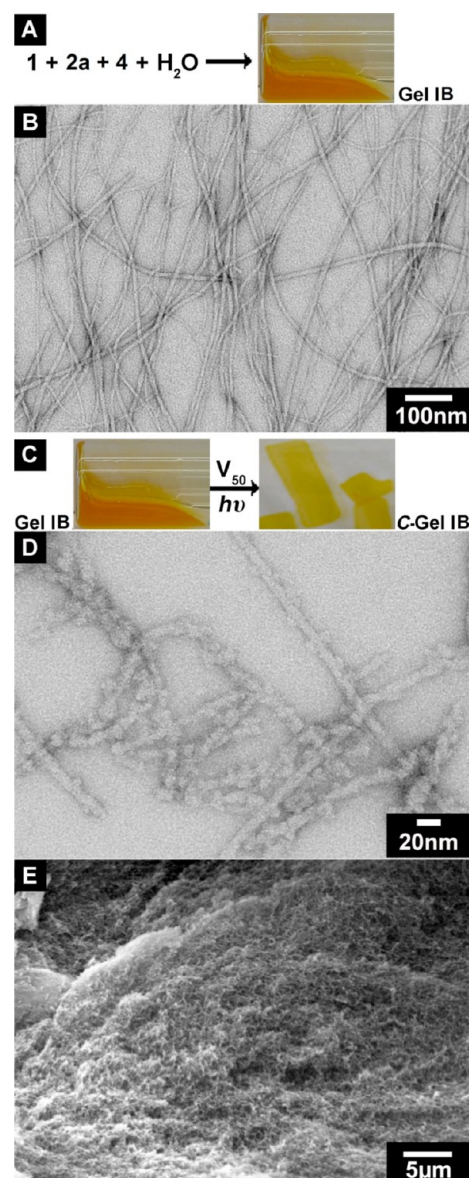


Figure 3. (A) Process for making molecular hydrogel (Gel IB) by self-assembly of **1** after addition of **1**, **2a**, and **4** to water and adjustment of the pH to 9. (B) TEM image of Gel IB. (C) Process for making cross-linked hydrogel C-Gel IB by addition of V_{50} (0.0092 mg) to the mixture with subsequent UV irradiation. (D) TEM image of the polymerized and cross-linked gel (C-Gel IB). (E) SEM image of C-Gel IB.

the width of the nanofibers (16 ± 2 nm, Figure 5D). The number of nodes and attachments along the nanofibers also increases significantly, which is consistent with the incorporation of more poly(NIPAAm) polymers and more cross-linkers. The entanglement due to the copolymerization gives an uneven distribution of pore sizes from 20 to 300 nm. SEM (Figure 5E) of C-gel ID shows that the pores of the network on its surface are about 200–300 nm in diameter, which implies substantial cross-linking after the self-assembly of the hydrogelators.

We tested the catalysts **2a** and **2b**, cross-linked gels, C-Gels IA, IB, IC, and ID, for chemical oscillation under the same initial conditions for the BZ reaction ($[\text{HNO}_3] = 0.8$ M; $[\text{NaBrO}_3] = 0.2$ M; $[\text{CH}_2(\text{COOH})_2] = 0.08$ M) at 20 °C. Figure 6 shows the periodic changes in the absorbance of the

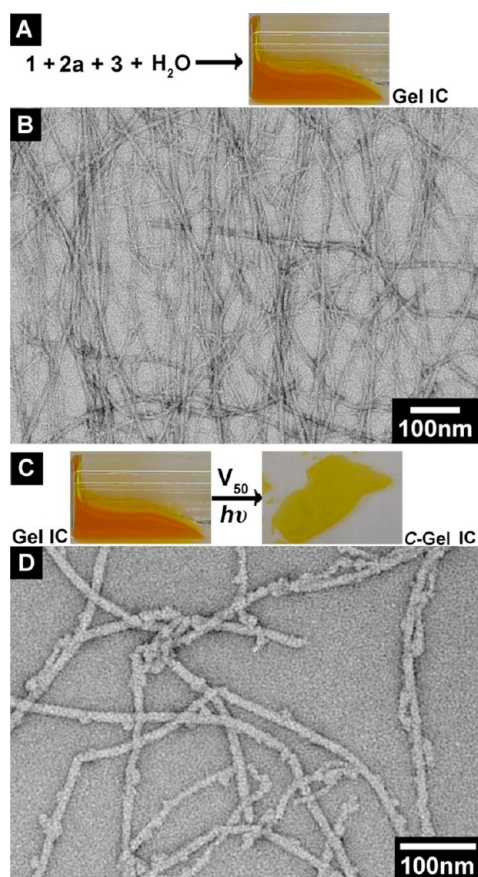


Figure 4. (A) Process for making molecular hydrogel (Gel IC) by self-assembly of **1** after addition of **1**, **2a**, and **3** to water and adjustment of the pH to 9. (B) TEM image of Gel IC. (C) Process for making cross-linked hydrogel C-Gel IC by the addition of V_{50} (0.0112 mg) to the mixture with subsequent UV irradiation. (D) TEM image of the polymerized and cross-linked gel (C-Gel IC).

catalysts. **2a** oscillated at 26 s/period and **2b** at 21 s/period. Compared to **2a**, **2b** has one more electron-withdrawing group on the bipyridyl ligand. This subtle difference may lead to faster oscillation of **2b** than that of **2a** under the same conditions. Relative to the oscillation frequency (20 s) of the catalyst (**5**)³³ used by Yoshida and others for the synthesis of BZ gels, **2a** oscillates relatively slowly. Figure 7 shows the periodic changes in the transmittance of these gels at constant temperature (20 °C) during the chemical oscillation. In the acidic BZ solution (pH < 1), all four gels exhibited only small volume changes during the chemical oscillation. The oscillation frequencies were different among these four gels under the same BZ conditions. C-Gel IA, IB, IC, and ID oscillated at 53, 56, 52, and 56 s/period, respectively, a longer cycle than that of the catalysts alone but a much shorter cycle than that of conventional poly(NIPAAm-Ru) gel (212 s/period) under the same conditions. This result indicates that not only the catalyst but also the polymer network determines the chemical oscillation behavior of the BZ gel. The polymer network, which controls the diffusion efficiency of the reactants into the gel, constructed by post-self-assembly cross-linking is much more porous than the poly(NIPAAm-Ru) gel. Modulating the porosity of the BZ gel could be a powerful way to tailor its chemical oscillation characteristics.

The procedure for making the type II gels is similar to that employed to form the type I gels, except that we use catalyst **2b**,

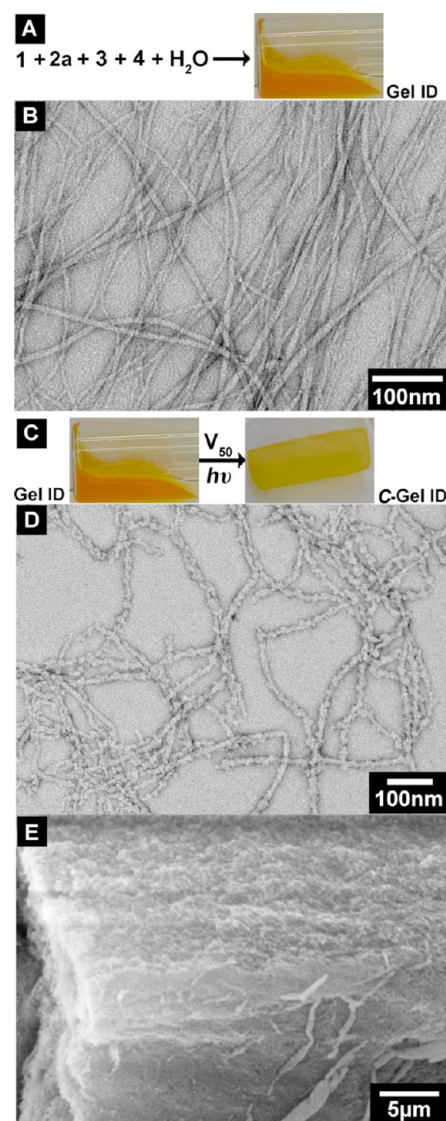


Figure 5. (A) Process for making molecular hydrogel (Gel ID) by self-assembly of **1** after the addition of **1**, **2a**, **3**, and **4** to water, and adjustment of the pH to 9. (B) TEM image of Gel ID. (C) Process for making cross-linked hydrogel C-Gel ID by addition of V_{50} (0.0140 mg) to the mixture with subsequent UV irradiation. (D) TEM image of the polymerized and cross-linked gel (C-Gel ID). (E) SEM image of C-Gel ID.

which can itself serve as the cross-linker. All type II gels, IIA, IIB, IIC, and IID, exhibit the appearance of soft, weak hydrogels. After the addition of initiator V_{50} and UV irradiation, these weak hydrogels are converted to thin film gels (Figure 8). The additional cross-linking effect from **2b** strengthens the type II hydrogels relative to their type I counterparts. The stronger cross-linking allows the gels to be cut easily into arbitrary shapes, such as the rectangles in Figure 8.

The oscillatory behavior of C-Gel IIA and C-Gel IIB under our standard BZ reaction conditions is shown in Figure 9. No obvious chemical oscillations were observed with C-Gel IIC and C-Gel IID. The average oscillation period of C-Gel IIA (45 s) is notably shorter than that of the type I gels. Compared with **2a**, which attaches to the nanofibers by an amide bond, **2b** partially embeds into the nanofibers, since one of the bipyridyl ligands is in the nanofibers. Especially after introducing **3** into the polymerization, **2b** may be wrapped more deeply into the gel

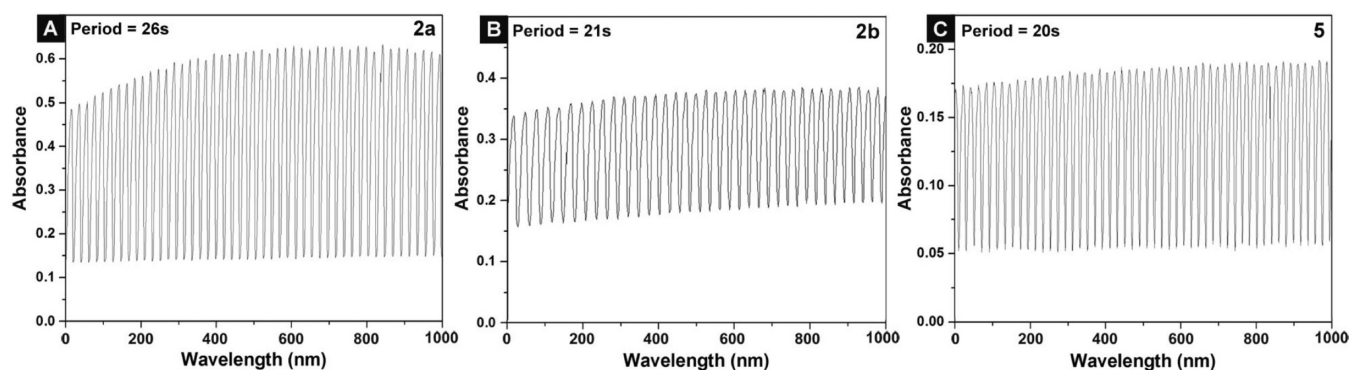


Figure 6. Oscillatory profiles of catalysts (A) 2a, (B) 2b, and (C) 5 under BZ condition.

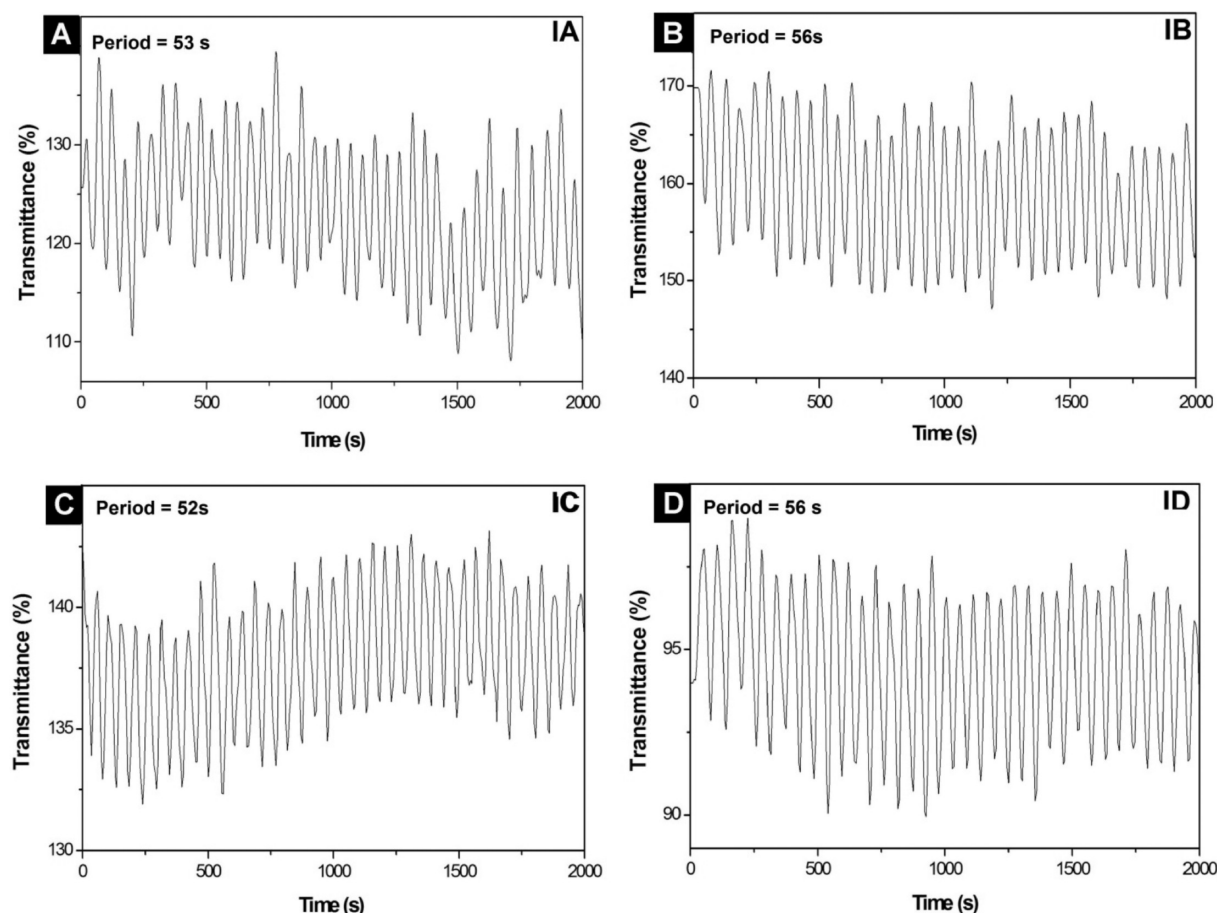


Figure 7. Oscillatory profiles of optical transmittance for C-Gels IA, IB, IC, and ID under BZ conditions.

network than 2a. This difference may contribute to the lack of chemical oscillation in C-Gel IIC and C-Gel IID. The faster oscillating behavior of C-Gel IIA may originate from the relatively faster oscillating behavior of catalyst 2b relative to 2a. The addition of BIS cross-linker in the preparation of C-Gel IIB slowed the oscillation compared to C-Gel IIA. The same trend also appeared in C-Gel I, which indicates that higher cross-linking density results in slower chemical oscillation. Like the type I gels, C-Gel IIA and C-Gel IIB exhibit only very small volume changes during the oscillation, even though the fluctuation of the polymer network creates local swelling and deswelling regions in the hydrogels. There is no simple correlation between the diameter of the nanofibers and the average pore size. Since the catalysts cross-link to the polymer

backbone and are wrapped in the gel network, the solubility difference of the Ru catalyst moiety, which couples with the oxidized and reduced states, remains minimal. These results suggest that the swelling–deswelling of the gel is negatively correlated with the period of the self-oscillation; that is, the volume change decreases as the frequency of oscillation increases.

CONCLUSION

We have developed a new type of chemical oscillatory system, which we use to study the BZ reaction in a series of polymeric hydrogels formed via post-self-assembly cross-linking. By introducing other monomer species into the system without compromising the self-assembled nanostructure, the post-self-

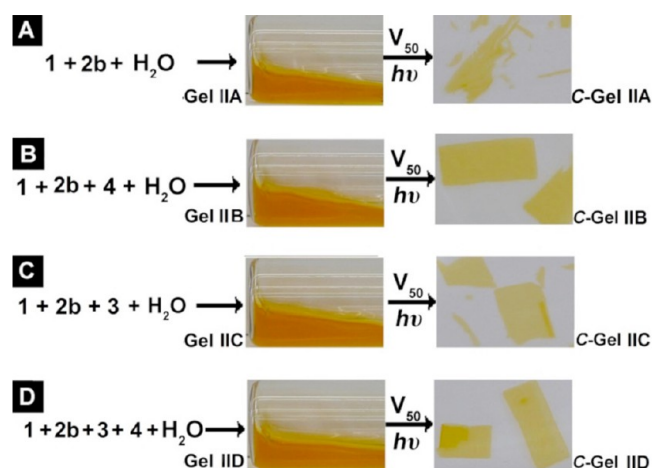


Figure 8. Process for making type II hydrogels via self-assembly and cross-linking, and optical images of the hydrogels before and after cross-linking. The compositions of the starting mixtures are given in Table 1. Quantities of water, V_{50} and length of UV irradiation are same as in Figure 2.

assembly cross-linking serves as a powerful approach for material synthesis with prearranged nanostructures. This work also implies that the engineering of molecular hydrogelators should allow the manipulation of self-assembled networks, including their pore sizes, for novel oscillatory gels. We designed and synthesized a new type of ruthenium catalyst that can also serve as a cross-linker to increase the cross-link density of the gel. The introduction of a cross-linkable hydrogelator not only provides a convenient method to integrate different catalysts into molecular nanofibers and preserve ordered matrices formed by self-assembly for oscillatory reactions, but also allows us to bring compositional modifications to polymeric networks by altering the concentration and type of ruthenium catalyst/cross-linker. By comparing structural characteristics with oscillatory profiles of hydrogels, the influence of ruthenium catalyst, cross-linker, and the molecular nanofibers provides useful insights for the development of future self-oscillatory soft materials.

■ ASSOCIATED CONTENT

■ Supporting Information

Details of synthesis and additional SEM images. This material is available free of charge via the Internet at <http://pubs.acs.org>.

■ AUTHOR INFORMATION

Corresponding Author

*E-mails: epstein@brandeis.edu, bux@brandeis.edu.

Notes

The authors declare no competing financial interest.

■ ACKNOWLEDGMENTS

This work was partially supported by grants from the Army Research Office (ARO 56735-MS), the National Science Foundation MRSEC Grant (DMR-0820492) and CHE-1012428 and start-up funds from Brandeis University. The TEM images were taken at the Brandeis EM facility.

■ REFERENCES

- (1) Zhang, Y.; Li, N.; Delgado, J.; Gao, Y.; Kuang, Y.; Fraden, S.; Epstein, I. R.; Xu, B. Post-Self-Assembly Cross-Linking of Molecular Nanofibers for Oscillatory Hydrogels. *Langmuir* **2012**, *28*, 3063–3066.
- (2) Nanda, J.; Adhikari, B.; Basak, S.; Banerjee, A. Formation of Hybrid Hydrogels Consisting of Tripeptide and Different Silver Nanoparticle-Capped Ligands: Modulation of the Mechanical Strength of Gel Phase Materials. *J. Phys. Chem. B* **2012**, *116*, 12235–12244.
- (3) Gao, Y.; Zhao, F.; Wang, Q. G.; Zhang, Y.; Xu, B. Small Peptide Nanofibers as the Matrices of Molecular Hydrogels for Mimicking Enzymes and Enhancing the Activity of Enzymes. *Chem Soc Rev* **2010**, *39*, 3425–3433.
- (4) Sadownik, J. W.; Ulijn, R. V. Dynamic Covalent Chemistry in Aid of Peptide Self-assembly. *Curr. Opin. Biotechnol.* **2010**, *21*, 401–411.
- (5) Yang, C. H.; Li, D. X.; Liu, Z.; Hong, G.; Zhang, J.; Kong, D. L.; Yang, Z. M. Responsive Small Molecular Hydrogels Based on Adamantane-Peptides for Cell Culture. *J. Phys. Chem. B* **2012**, *116*, 633–638.
- (6) Qiao, Y.; Lin, Y. Y.; Yang, Z. Y.; Chen, H. F.; Zhang, S. F.; Yan, Y.; Huang, J. B. Unique Temperature-Dependent Supramolecular Self-Assembly: From Hierarchical 1D Nanostructures to Super Hydrogel. *J. Phys. Chem. B* **2010**, *114*, 11725–11730.
- (7) Debnath, S.; Shome, A.; Das, D.; Das, P. K. Hydrogelation through Self-Assembly of Fmoc-Peptide Functionalized Cationic Amphiphiles: Potent Antibacterial Agent. *J. Phys. Chem. B* **2010**, *114*, 4407–4415.

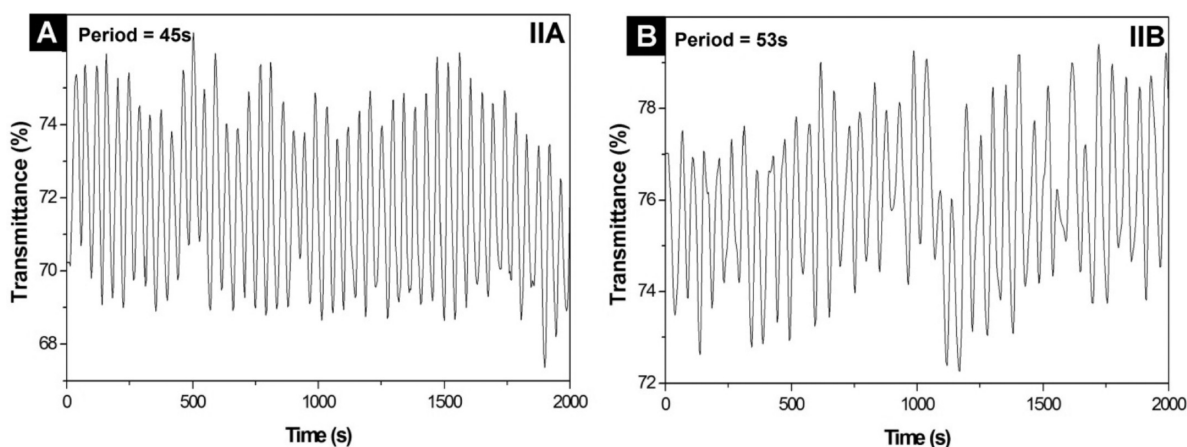


Figure 9. Oscillatory profiles of optical transmittance for C-Gel IIA, and C-Gel IIB under BZ condition.

- (8) Ge, J.; Lu, D. N.; Wang, J.; Yan, M.; Lu, Y. F.; Liu, Z. Molecular Fundamentals of Enzyme Nanogels. *J. Phys. Chem. B* **2008**, *112*, 14319–14324.
- (9) Dudowicz, J.; Douglas, J. F.; Freed, K. F. Self-Assembly by Mutual Association: Basic Thermodynamic Properties. *J. Phys. Chem. B* **2008**, *112*, 16193–16204.
- (10) Mitra, R. N.; Das, D.; Roy, S.; Das, P. K. Structure and Properties of Low Molecular Weight Amphiphilic Peptide Hydrogelators. *J. Phys. Chem. B* **2007**, *111*, 14107–14113.
- (11) Bieser, A. M.; Tiller, J. C. Structure and Properties of an Exceptional Low Molecular Weight Hydrogelator. *J. Phys. Chem. B* **2007**, *111*, 13180–13187.
- (12) Kapral, R. Oscillating Chemical Reactions: Oscillations and Traveling Waves in Chemical Systems. *Science* **1985**, *229*, 852–853.
- (13) Epstein, I. R.; Pojman, J. A. *An Introduction to Nonlinear Chemical Dynamics: Oscillations, Waves, Patterns, and Chaos*; Oxford University Press: New York, 1998.
- (14) Belousov, B. P. In *Med. Publ.* Moscow, 1959.
- (15) Bansagi, T., Jr.; Vanag, V. K.; Epstein, I. R. Tomography of Reaction-Diffusion Microemulsions Reveals Three-Dimensional Turing Patterns. *Science (Washington, DC, U.S.)* **2011**, *331*, 1309–1312.
- (16) Agladze, K. I.; Krinsky, V. I. Multi-armed Vortices in an Active-Chemical Medium. *Nature* **1982**, *296*, 424–426.
- (17) Yashin, V. V.; Balazs, A. C. Pattern Formation and Shape Changes in Self-oscillating Polymer Gels. *Science* **2006**, *314*, 798–801.
- (18) Epstein, I. R.; Pojman, J. A. Nonlinear Dynamics Related to Polymeric Systems—Overview. *Chaos* **1999**, *9*, 255–259.
- (19) Yoshida, R.; Takahashi, T.; Yamaguchi, T.; Ichijo, H. Self-oscillating gel. *J. Am. Chem. Soc.* **1996**, *118*, 5134–5135.
- (20) Yoshida, R.; Takahashi, T.; Yamaguchi, T.; Ichijo, H. Self-oscillating gels. *Adv. Mater.* **1997**, *9*, 175–178.
- (21) Vanag, V. K.; Yang, L. F.; Dolnik, M.; Zhabotinsky, A. M.; Epstein, I. R. Oscillatory Cluster Patterns in a Homogeneous Chemical System with Global Feedback. *Nature* **2000**, *406*, 389–391.
- (22) Szalai, I.; Oslonovitch, J.; Forsterling, H. D. Oscillations in the Bromomalonic Acid/Bromate System Catalyzed by [Ru(phen)(3)](2+). *J. Phys. Chem. A* **2000**, *104*, 1495–1498.
- (23) Ruoff, P.; Varga, M.; Koros, E. How Bromate Oscillators Are Controlled. *Acc. Chem. Res.* **1988**, *21*, 326–332.
- (24) Schild, H. G. Poly (N-Isopropylacrylamide)—Experiment, Theory and Application. *Prog. Polym. Sci.* **1992**, *17*, 163–249.
- (25) Shinohara, S.; Seki, T.; Sakai, T.; Yoshida, R.; Takeoka, Y. Chemical and Optical Control of Peristaltic Actuator Based on Self-oscillating Porous Gel. *Chem. Commun.* **2008**, 4735–4737.
- (26) Chen, I. C.; Kuksenok, O.; Yashin, V. V.; Moslin, R. M.; Balazs, A. C.; Van Vliet, K. J. Shape- and Size-Dependent Patterns in Self-Oscillating Polymer Gels. *Soft Matter* **2011**, *7*, 3141–3146.
- (27) Wang, T. X.; Xu, A. W.; Colfen, H. Formation of Self-Organized Dynamic Structure Patterns of Barium Carbonate Crystals in Polymer-Controlled Crystallization. *Angew. Chem., Int. Ed.* **2006**, *45*, 4451–4455.
- (28) Yuan, P. X.; Kuksenok, O.; Gross, D. E.; Balazs, A. C.; Moore, J. S.; Nuzzo, R. G. UV Patternable Thin Film Chemistry for Shape and Functionally Versatile Self-Oscillating Gels. *Soft Matter* **2013**, *9*, 1231–1243.
- (29) Zhang, Y.; Kuang, Y.; Gao, Y. A.; Xu, B. Versatile Small-Molecule Motifs for Self-Assembly in Water and the Formation of Biofunctional Supramolecular Hydrogels. *Langmuir* **2011**, *27*, 529–537.
- (30) Younathan, J. N.; Jones, W. E.; Meyer, T. J. Energy-Transfer and Electron-Transfer Shuttling by a Soluble, Bifunctional Redox Polymer. *J. Phys. Chem., U.S.* **1991**, *95*, 488–492.
- (31) Zeyer, K. P.; Schneider, F. W. Periodicity and Chaos in Chemiluminescence: The Ruthenium-catalyzed Belousov-Zhabotinsky Reaction. *J. Phys. Chem. A* **1998**, *102*, 9702–9709.
- (32) Gao, Y.; Yang, Z. M.; Kuang, Y.; Ma, M. L.; Li, J. Y.; Zhao, F.; Xu, B. Enzyme-Instructed Self-Assembly of Peptide Derivatives to Form Nanofibers and Hydrogels. *Biopolymers* **2010**, *94*, 19–31.
- (33) Yoshida, R. Self-Oscillating Gels Driven by the Belousov-Zhabotinsky Reaction as Novel Smart Materials. *Adv. Mater. (Weinheim, Ger.)* **2010**, *22*, 3463–3483.